nature methods

BRIEF COMMUNICATION

https://doi.org/10.1038/s41592-018-0084-1

Corrected: Publisher correction

Single-DNA electron spin resonance spectroscopy in aqueous solutions

Fazhan Shi[1,2,3,5], Fei Kong[1,2,3,5], Pengju Zhao[1,3,5], Xiaojun Zhang[4], Ming Chen[1,3], Sanyou Chen[1,3], Qi Zhang[1,3], Mengqi Wang[1,3], Xiangyu Ye[1,2,3], Zhecheng Wang[1,3], Zhuoyang Qin[1,3], Xing Rong[1,2,3], Jihu Su[1,2,3], Pengfei Wang[1,2,3], Peter Z. Qin[4*] and Jiangfeng Du[1,2,3*]

Magnetic resonance spectroscopy of single biomolecules under near-physiological conditions could substantially advance understanding of their biological function, but this approach remains very challenging. Here we used nitrogen-vacancy centers in diamonds to detect electron spin resonance spectra of individual, tethered DNA duplexes labeled with a nitroxide spin label in aqueous buffer solutions at ambient temperatures. This work paves the way for magnetic resonance studies on single biomolecules and their intermolecular interactions in native-like environments.

Owing to the enormous power of magnetic resonance spectroscopy, including nuclear magnetic resonance and electron spin resonance (ESR), for investigations of molecular structure and dynamics, intensive efforts are being devoted to the development of single-spin magnetic resonance spectroscopy, and rapid progress is being made[1]. The use of nitrogen-vacancy (NV) centers in diamonds is a promising avenue for single-spin detection[2–4]. For example, we previously reported single-molecule ESR spectroscopy of proteins labeled with a nitroxide spin label and embedded in a poly-lysine layer at diamond surfaces[5]. In all prior NV work, the target has been either embedded in the diamond lattice[6–8] or fixed at the diamond surface[5,9,10]. However, the majority of biomolecules function in aqueous solution under ambient temperature, where they undergo a range of motions. NV detection of single molecules under near-physiological conditions presents considerable additional challenges compared with studies carried out at a stationary solid phase, and has not yet been reported.

We report here two technical advancements to allow ESR measurements of single spin-labeled DNAs in aqueous solution at ambient temperature. We implemented a diamond pillar array design (Fig. 1a, Supplementary Note 1, and Methods), which reduced the detection time for an ESR spectrum by approximately one order compared with that in our previous work on immobilized proteins[5]. This enabled us to record multiple ESR spectra before the labels were quenched by laser irradiation[11]. Furthermore, to confine a spin-labeled DNA duplex within the ~10-nm detection range from a shallowly embedded NV, we adapted a chemical tethering scheme[12] in which a non-labeled DNA was covalently attached to the diamond surface, then hybridized with a complementary strand with a spectroscopic label (Fig. 1b and Methods). Atomic force microscopy imaging indicated that the tethered DNA formed an evenly distributed single layer at the diamond surface (Supplementary Note 2). Characterizations using a Cy3-labeled DNA complementary strand and fluorescence confocal microscopy demonstrated that DNA-duplex localization depends on the presence of the covalently attached non-labeled strand. Under the experimental conditions used in this work, spacing between the DNA duplexes was approximately 21 nm (Supplementary Note 2). This resulted in a 14% probability of a single DNA duplex being located within the detection range of an NV sensor, whereas the probability of detecting two or more DNA duplexes was 1% (Supplementary Note 3). Thus, the signal detected from a single NV center was predominantly from a single DNA duplex.

Using the tethering scheme, we localized DNA duplexes with a covalently attached nitroxide spin label (designed as R5[13]) at the diamond pillar surface (Fig. 1b,c). We detected an ESR spectrum by using a double electron–electron resonance pulse sequence[5] (Fig. 1d, Supplementary Note 3). Figure 2a shows an example of an NV-detected spectrum of a ^{14}N-R5-labeled DNA obtained with an external magnetic field B_0 of 809 G, with three peaks. The isotropic hyperfine coupling, measured between the two side peaks, was $A_{iso}^{14N} = 38.4 \pm 1.2$ MHz, similar to that obtained from an ensemble measurement (Fig. 2b and Supplementary Note 4) (A_{iso} is discussed further below). Note that while both the NV-detected spectrum (Fig. 2a, top) and the ensemble spectrum (Fig. 2b) had an expected three-line pattern due to hyperfine interactions between the electron spin ($S = 1/2$) and the ^{14}N nucleic spin ($I = 1$), it is likely that the center peak of the NV-detected spectrum (gyromagnetic ratio of 2.801 ± 0.002 MHz/G or g-factor $= 2.001 \pm 0.002$) was composed of signals from both ^{14}N-R5 and paramagnetic diamond surface defects[8], which have similar g-factors and therefore were not separable in the measurements (Supplementary Note 3). In agreement with this interpretation, the two side peaks disappeared after prolonged laser irradiation, which has been reported to quench the nitroxide[11] (Fig. 2a, bottom). Furthermore, for diamond surfaces not exposed to spin-labeled DNAs, the NV-detected spectra showed only one peak without splitting (Supplementary Note 3). Together, observations of the side peaks in the NV-detected spectra indicated that we had detected single spin-labeled DNA molecules by magnetic resonance in solution at ambient temperature.

To further verify the detection of nitroxide-labeled DNAs, we substituted the ^{14}N-R5 label with ^{15}N-R5, which we expected to change the hyperfine coupling (Supplementary Note 4). Indeed, before nitroxide decomposition, the NV-detected spectrum showed two side peaks (Fig. 2c, top) that gave an A_{iso}^{15N} value of 56.6 MHz. The

[1]CAS Key Laboratory of Microscale Magnetic Resonance and Department of Modern Physics, University of Science and Technology of China (USTC), Hefei, China. [2]Hefei National Laboratory for Physical Sciences at the Microscale, USTC, Hefei, China. [3]Synergetic Innovation Center of Quantum Information and Quantum Physics, USTC, Hefei, China. [4]Department of Chemistry, University of Southern California, Los Angeles, CA, USA. [5]These authors contributed equally to this work: Fazhan Shi, Fei Kong, Pengju Zhao. *e-mail: pzq@usc.edu; djf@ustc.edu.cn

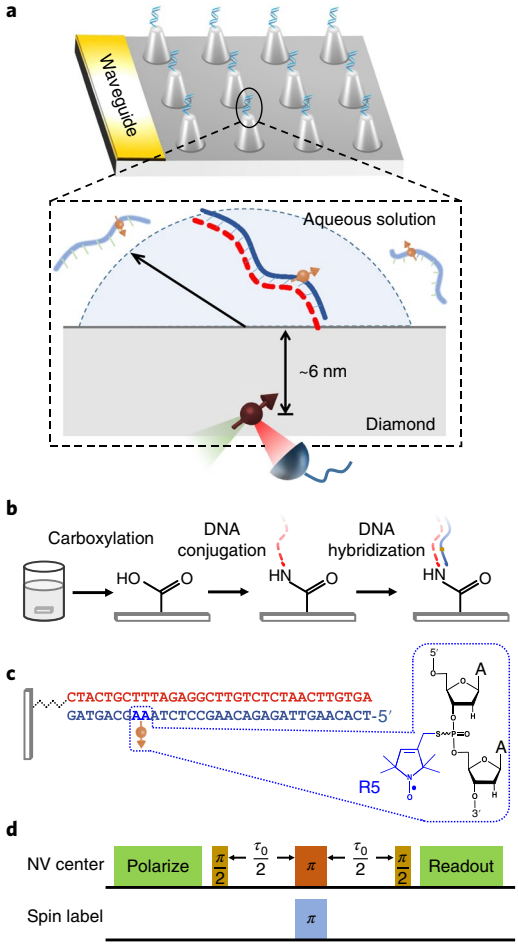

Fig. 1 | Experimental setup. a, Top, schematic of diamond pillars with surface-tethered DNA. Bottom, a surface-tethered DNA strand (red dashed line) hybridizes with a strand (blue solid line) containing a spin label (orange arrow) to localize a spin-labeled duplex within the detection volume of an NV (dark red arrow). **b**, The DNA-tethering scheme. A 5′ -NH_2-modified strand (red dashed line) reacts with the carboxylate groups at the diamond surface, then hybridizes with a complementary strand (blue line). **c**, The tethered DNA duplex with an R5 label (orange arrow) 8 bp away from the linker. The structure on the right shows R5 with either ^{14}N or ^{15}N at the pyrroline ring. **d**, Double electron–electron resonance pulse sequence for target spin detection.

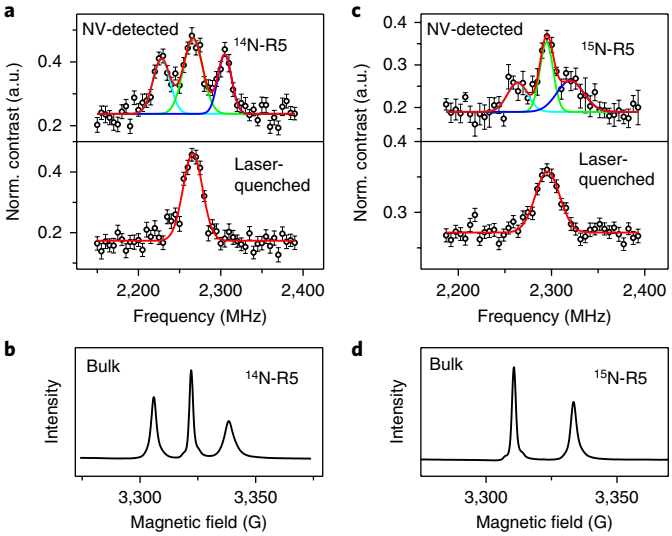

Fig. 2 | ESR spectra detected at single-molecule and bulk levels. a, NV-detected spectrum of a single ^{14}N-R5-labeled DNA (circles, experimental values; lines, Gaussian peak fits). Top, an early-time-point spectrum with three peaks. The two side peaks (2,228.0 ± 1.3 and 2,304.8 ± 1.0 MHz) give a measured $2A_{iso}$ value of 76.8 ± 2.3 MHz. The center peak (2,266.4 ± 1.0 MHz) includes signals from the ^{14}N-R5 and paramagnetic surface defects. Bottom, spectrum observed after laser-quenching of the nitroxide. Only one peak (2,266.4 ± 1.0 MHz) corresponding to the defects is present. Data were obtained from 0.8 million (top) and 1.2 million (bottom) repetitions and are shown as mean (dots) ± s.e.m. **b**, A representative ensemble X-band spectrum of the corresponding ^{14}N-R5-labeled duplex, showing the three-peak pattern expected from hyperfine interaction between the electron spin (S = 1/2) and the ^{14}N nucleus (I = 1). Experiments were repeated three times independently, and spectra obtained were highly similar with $2A_{iso}$ = 91.6 ± 0.3 MHz. **c**, NV-detected ESR spectrum of single DNA duplexes labeled with ^{15}N-R5. The two side peaks, which were observed initially (top) but disappeared within 1 h (bottom), centered respectively at 2,263.5 ± 2.5 and 2,320.1 ± 5.8 MHz, yielding an A_{iso} value of 56.6 ± 8.3 MHz. The center peak (2,294.6 ± 1.2 MHz) in both plots represents the surface defects. Data shown were obtained from 4 million (top) and 20 million (bottom) repetitions and are shown as mean (dots) ± s.e.m. **d**, A representative ensemble X-band spectrum of the corresponding ^{15}N-R5-labeled duplex, showing the two-peak pattern expected from hyperfine interaction between the electron spin (S = 1/2) and the ^{15}N nucleus (I = 1/2). Experiments were repeated three times independently, and spectra obtained were highly similar, with A_{iso} = 64.3 ± 0.2 MHz. a.u., arbitrary units.

obtained $A_{iso}^{^{15}N}/A_{iso}^{^{14}N}$ ratio of 1.47 ± 0.26 is consistent with the gyromagnetic ratio $\gamma_{^{15}N}/\gamma_{^{14}N}$ of 1.40, thus confirming NV detection of spin-labeled DNA. Note that whereas the ^{15}N-R5-labeled DNA showed the expected two-line pattern in ensemble measurements (Fig. 2d and Supplementary Note 4), the NV-detected early-time-point spectrum shows three peaks (Fig. 2c, top). We assigned the center peak to the paramagnetic diamond-surface defects, which persisted upon prolonged laser radiation (Fig. 2c, bottom). Overall, the ^{14}N and ^{15}N data unambiguously demonstrate the detection of an external nitroxide-labeled DNA.

Analyses of NV-detected spectra led to a number of interesting observations. First, the A_{iso} values varied by ~12%, reflecting heterogeneity among the individual molecules (Supplementary Note 3). All A_{iso} values measured from NV-detected spectra were smaller (6–16%) than that measured in the bulk solution (Supplementary Note 3). It is known that a more hydrophobic environment, such as that at the diamond surface, reduces hyperfine couplings[14]. The A_{iso} variations may reflect heterogeneity of the polarity profile at the individual DNA duplexes, although many other factors (e.g., spin label dynamics, local electrostatics) cannot be completely ruled out (Supplementary Note 5). A second observation is that the NV-detected DNA spectrum showed sharp side peaks with small line-shape variations (Fig. 2 and Supplementary Note 3). This differs from spectra from proteins fixed in the poly-lysine layer[5], and reflects the high degree of motion expected from DNA in solution (Supplementary Note 5). Analyses showed that the side peaks of the NV-detected spectrum were best matched in simulations in which the label underwent an isotropic rotation with a rotational correlation time τ of 1.0 ns (Supplementary Note 5), which is similar to that reported in bulk solution measurements of R5-labeled DNAs tethered to nanodiamonds[15]. Overall, these results indicate that analysis of an NV-detected single-molecule spectrum provides information on the local environment and motion dynamics of a biomolecule. However, more work, including studies with substantially increased numbers of observed spectra, will be required in order to retrieve

functional information, such as variations in DNA conformation and interactions between DNA and proteins or ligands.

In conclusion, we developed NV-based methods that enabled us to carry out ESR spectroscopic analyses of single spin-labeled DNA molecules in aqueous solution at ambient temperature. As demonstrated by developments in other fields (for example, fluorescent spectroscopy[16] and force microscopy[17]), single-molecule measurements can lead to drastic advances in the understanding of function. The work reported here represents a step forward toward single-molecule magnetic resonance investigation of structure, dynamics, and interaction of biomolecules in their native environments.

Methods

Methods, including statements of data availability and any associated accession codes and references, are available at https://doi.org/10.1038/s41592-018-0084-1.

Received: 6 November 2017; Accepted: 11 June 2018;
Published online: 6 August 2018

References

1. Wrachtrup, J. & Finkler, A. *J. Magn. Reson.* **269**, 225–236 (2016).
2. Balasubramanian, G. et al. *Nature* **455**, 648–651 (2008).
3. Maze, J. R. et al. *Nature* **455**, 644–647 (2008).
4. Degen, C. L., Reinhard, F. & Cappellaro, P. *Rev. Mod. Phys.* **89**, 035002 (2017).
5. Shi, F. et al. *Science* **347**, 1135–1138 (2015).
6. Shi, F. et al. *Phys. Rev. B* **87**, 195414 (2013).
7. Grinolds, M. S. et al. *Nat. Phys.* **9**, 215–219 (2013).
8. Grinolds, M. S. et al. *Nat. Nanotechnol.* **9**, 279–284 (2014).
9. Grotz, B. et al. *New J. Phys.* **13**, 055004 (2011).
10. Sushkov, A. O. et al. *Nano Lett.* **14**, 6443–6448 (2014).
11. Schlipf, L. et al. *Sci. Adv.* **3**, e1701116 (2017).
12. Lovchinsky, I. et al. *Science* **351**, 836–841 (2016).
13. Tangprasertchai, N. S. et al. *Methods Enzymol.* **564**, 427–453 (2015).
14. Kurad, D., Jeschke, G. & Marsh, D. *Biophys. J.* **85**, 1025–1033 (2003).
15. Akiel, R. D. et al. *J. Phys. Chem. B* **120**, 4003–4008 (2016).
16. Zhuang, X. et al. *Science* **288**, 2048–2051 (2000).
17. Rugar, D., Budakian, R., Mamin, H. J. & Chui, B. W. *Nature* **430**, 329–332 (2004).

Acknowledgements

This work was supported in part by the National Key R&D Program of China (grant 2016YFA0502400 to F.S.; grant 2018YFA0306600 to J.D.), the National Natural Science Foundation of China (grants 81788104, 11227901, and 11761131011 to J.D.; grants 31470835, 91636217, and 11722544 to F.S.; grant 21328101 to P.Z.Q.), CAS (grants XDB01030400 and QYZDY-SSW-SLH004 to J.D.; grant YIPA2015370 to F.S.), the CEBioM (F.S.), the Fundamental Research Funds for the Central Universities (grant WK2340000064 to F.S.; grant WK2030040088 to P.W.), the China Postdoctoral Science Foundation (grant BX20180294 to F.K.; grants BX201700230 and 2017M622001 to Q.Z.) and the US National Science Foundation (grants CHE-1213673, MCB-1716744, and MCB-1818107 to P.Z.Q.).

Author contributions

J.D. supervised the entire project. J.D., F.S., and P.Z.Q. designed the experiments. F.K., P.Z., and F.S. performed the experiments. X.Z. and P.Z.Q. prepared the DNA duplex. X.Z., M.C., X.R., J.S., and P.Z.Q. measured the ensemble data. P.Z., M.C., Z.W., S.C., and P.Z.Q. carried out the chemical bonding process. M.W., X.Y., and P.W. fabricated the pillar and conducted atomic force microscopy imaging. Q.Z. tested the coherence of NVs. F.K. and Z.Q. performed calculations. F.S., F.K., P.Z., P.Z.Q., and J.D. wrote the manuscript. All authors discussed the results and commented on the manuscript.

Competing interests

The authors declare no competing interests.

Additional information

Supplementary information is available for this paper at https://doi.org/10.1038/s41592-018-0084-1.

Reprints and permissions information is available at www.nature.com/reprints.

Correspondence and requests for materials should be addressed to P.Z.Q. or J.D.

Publisher's note: Springer Nature remains neutral with regard to jurisdictional claims in published maps and institutional affiliations.

Methods

Diamond sensors. All diamonds used were obtained commercially (Element Six, Inc., UK), 100-oriented, and electronic-grade. NV centers were created[18] by implantation of 4-keV $^{15}N^{2+}$ ions with a dose of $1\times10^{11}\,cm^{-2}$. The diamond nanopillars were fabricated by electron beam lithography and reactive ion etching to enhance the photon-collection efficiency[19]. First negative electron-beam-resisting hydrogen silsesquioxane (HSQ) was spun on the diamond to a thickness of 350 nm. The HSQ layer was patterned by electron-beam writing followed by tetramethyl ammonium hydroxide (4%) development. The nanopillars were then formed after reactive ion etching with mixed CHF_3 and O_2, with the etching depth at ~400 nm. Finally, hydrofluoric acid was used to remove the HSQ resisting layer.

DNA samples. All DNAs were produced by solid-phase chemical synthesis and obtained commercially (Integrated DNA Technologies, Inc., Skokie, IL, USA and Sangon Biotech, Inc., Shanghai, China). The DNA strand for covalent attachment to the diamond surface (NH_2-DNA) had a sequence of 5′-NH_2-CTACTGCTTTAGAGGCTTGTCTCTAACTTGTGA-3′, with "NH_2" representing an amino-modifier C6 at the 5′ terminus. The complementary DNA strand (designated as s1) had a sequence of 5′-TCACAAGTTAGAGACAAGCCTCTAAAGCAGTAG-3′. The 5′ Cy3-modified s1 strand (Cy3-s1) was obtained commercially. The R5 spin label (1-oxyl-2,2,5,5-tetramethyl-pyrroline) (Fig. 1c) was attached to phosphorothioate-modified s1 strands according to previously reported protocols and purified by high-performance liquid chromatography[13,20]. The R5-labeling efficiency was estimated as >90% by a spin-counting procedure[21].

Covalent attachment of DNA at the diamond surface. Prior to DNA attachment, we cleaned the diamond surface in four steps: (i) submersion in Piranha solution (2:1 mixture of concentrated H_2SO_4 and 30% hydrogen peroxide) at 150 °C for at least 4 h; (ii) submersion in concentrated HNO_3 at 90 °C for 1 h; (iii) submersion in 1 M NaOH at 90 °C for 1 h; and (iv) submersion in 1 M HCl at 90 °C for 1 h. After each step, the diamond was rinsed with deionized water. After the surface was cleaned, a freshly prepared solution containing 10 μM NH_2-DNA, 5 mM EDC (1-ethyl-3-(3-dimethylaminopropyl) carbodiimide hydrochloride; Sigma-Aldrich (39391-50 ML)) in 100 mM MES (2-(*N*-morpholino)ethanesulfonic acid, pH 5.0) was applied to the diamond surface. The reaction was allowed to proceed at room temperature for 30 min, after which the diamond surface was rinsed with deionized water. We repeated this procedure three times to maximize the amount of DNA tethered to the diamond surface.

To hybridize a complementary strand to a tethered DNA strand, we prepared a 2 μM Cy3 or R5-labeled s1 strand solution in 100 mM NaCl, and added 2 μL of this solution to the diamond surface bearing tethered DNA. After allowing the reaction to proceed in the dark for 10 h at room temperature, we rinsed the diamond surface with PBS at least three times before carrying out either ESR detection using NV centers (see below) or fluorescent and atomic force microscopy measurements (Supplementary Note 2).

NV-center-based ESR spectroscopy. The measurements were carried out on an in-house-built system according to previously reported procedures[5]. Briefly, a 532-nm green laser was used to illuminate the NV centers for initialization and readout. The external magnetic field was set at $B_0 = 809$ G. The microwave (MW) and radio frequency (RF) irradiations were generated by an arbitrary waveform generator (Agilent; M8190a), amplified (Mini-circuits; ZHL-20W-13+ for MW, ZHL16W-43+ for RF), and delivered by a coplanar waveguide fabricated on a glass substrate. Double electron–electron resonance pulse sequences were used to detect the weak signal from the spin labels (Fig. 1d). The MW pulses, which manipulated the NV center for detection, were set at approximately 0.6 GHz. The RF pulse, which manipulated the spin label, was scanned between 2.15 and 2.39 GHz. The π-pulse widths of the MW and RF pulses were approximately 11 ns and 50 ns, respectively, corresponding to Rabi frequencies around 45 MHz and 10 MHz, respectively. The phase-accumulating duration τ_0 between the MW $\pi/2$ pulses was 4 μs (see Supplementary Note 3 for more details). We measured each NV-detected spectrum by repeating the pulse sequence (Fig. 1d) until laser quenching of the nitroxide or until a sufficient signal-to-noise ratio was obtained, and we reported the number of repetitions with the corresponding spectrum. The detected spectral signals were normalized by the amplitude of Rabi oscillations.

Reporting Summary. Further information on research design is available in the Nature Research Reporting Summary linked to this article.

Code availability. Customized codes for ESR spectral simulation and data analysis are available from the corresponding authors upon reasonable request.

Data availability. Data supporting the findings of this study are available within the paper and its Supplementary Information, and from the corresponding authors upon reasonable request. Source data for Fig. 2 are available online.

References

18. Pezzagna, S. et al. *New J. Phys.* **12**, 065017 (2010).
19. Hausmann, B. J. M. et al. *New J. Phys.* **13**, 045004 (2011).
20. Qin, P. Z. et al. *Nat. Protoc.* **2**, 2354–2365 (2007).
21. Zhang, X., Cekan, P., Sigurdsson, S. T. & Qin, P. Z. *Methods Enzymol.* **469**, 303–328 (2009).

nature research

Corresponding author(s): djf@ustc.edu.cn; pzq@usc.edu

Reporting Summary

Nature Research wishes to improve the reproducibility of the work that we publish. This form provides structure for consistency and transparency in reporting. For further information on Nature Research policies, see Authors & Referees and the Editorial Policy Checklist.

Statistical parameters

When statistical analyses are reported, confirm that the following items are present in the relevant location (e.g. figure legend, table legend, main text, or Methods section).

n/a	Confirmed	
☐	☒	The exact sample size (*n*) for each experimental group/condition, given as a discrete number and unit of measurement
☐	☒	An indication of whether measurements were taken from distinct samples or whether the same sample was measured repeatedly
☒	☐	The statistical test(s) used AND whether they are one- or two-sided *Only common tests should be described solely by name; describe more complex techniques in the Methods section.*
☒	☐	A description of all covariates tested
☒	☐	A description of any assumptions or corrections, such as tests of normality and adjustment for multiple comparisons
☒	☐	A full description of the statistics including central tendency (e.g. means) or other basic estimates (e.g. regression coefficient) AND variation (e.g. standard deviation) or associated estimates of uncertainty (e.g. confidence intervals)
☒	☐	For null hypothesis testing, the test statistic (e.g. *F*, *t*, *r*) with confidence intervals, effect sizes, degrees of freedom and *P* value noted *Give P values as exact values whenever suitable.*
☒	☐	For Bayesian analysis, information on the choice of priors and Markov chain Monte Carlo settings
☒	☐	For hierarchical and complex designs, identification of the appropriate level for tests and full reporting of outcomes
☒	☐	Estimates of effect sizes (e.g. Cohen's *d*, Pearson's *r*), indicating how they were calculated
☐	☒	Clearly defined error bars *State explicitly what error bars represent (e.g. SD, SE, CI)*

Our web collection on statistics for biologists may be useful.

Software and code

Policy information about availability of computer code

Data collection	Programs written and run in LabView 2012 were used for data collection in this study.
Data analysis	Programs with customized codes, written and run in Matlab R2016b, were used to analyze the single DNA ESR spectra. The algorithms of the customized code was described in Supplementary Note 5.B. The code is available upon request from the corresponding author, as we have indicated in Code Availability.

For manuscripts utilizing custom algorithms or software that are central to the research but not yet described in published literature, software must be made available to editors/reviewers upon request. We strongly encourage code deposition in a community repository (e.g. GitHub). See the Nature Research guidelines for submitting code & software for further information.

Data

Policy information about availability of data

All manuscripts must include a data availability statement. This statement should provide the following information, where applicable:

- Accession codes, unique identifiers, or web links for publicly available datasets
- A list of figures that have associated raw data
- A description of any restrictions on data availability

Data supporting the findings of this study are available within the article and its Supplementary Information file, and from the corresponding authors upon reasonable request. Source data for main-text figures are available online.

Field-specific reporting

Please select the best fit for your research. If you are not sure, read the appropriate sections before making your selection.

☒ Life sciences ☐ Behavioural & social sciences ☐ Ecological, evolutionary & environmental sciences

For a reference copy of the document with all sections, see nature.com/authors/policies/ReportingSummary-flat.pdf

Life sciences study design

All studies must disclose on these points even when the disclosure is negative.

Sample size	As detailed in Supplementary Note 3.B, the probability of a single DNA resided in the detection area of the NV center is ~14%. So measurements performed on tens of individual NV centers were sufficient to acquire the signal of single DNA.
Data exclusions	No data were excluded.
Replication	Experimental findings were reliably reproduced. Relevant information on repetition and reproducibility for each experiment has been described in the corresponding section (i.e., figure legends).
Randomization	Randomization was not relevant to this study, because no experimental groups were formed.
Blinding	Blinding was not relevant to this study, because no group allocation was performed.

Reporting for specific materials, systems and methods

Materials & experimental systems

n/a	Involved in the study
☒	☐ Unique biological materials
☒	☐ Antibodies
☒	☐ Eukaryotic cell lines
☒	☐ Palaeontology
☒	☐ Animals and other organisms
☒	☐ Human research participants

Methods

n/a	Involved in the study
☒	☐ ChIP-seq
☒	☐ Flow cytometry
☒	☐ MRI-based neuroimaging